Lab Notes

Editors
Thomas M. Moses | Shane F. McClure

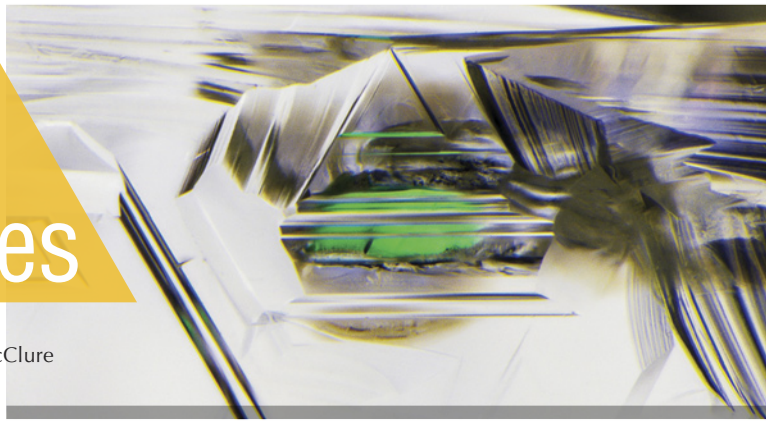

Color-Zoned Cat's-Eye CHRYSOBERYL

Chatoyancy occurs when light is reflected from certain oriented inclusions in a cabochon-cut gemstone. To be chatoyant, a group of fibers or needles or other reflective inclusions must be oriented parallel to the cabochon base. Usually these fibers and/or needles are dense and included throughout the stone, but occasionally there are cases with localized distribution of such inclusions.

GIA's Tokyo laboratory examined a brownish green cabochon set in a ring with numerous near-colorless round and marquise brilliant cut accent stones. The center stone showed pleochroism and a spot RI reading of 1.75. The spectrum observed with a handheld spectroscope clearly showed the 444 nm band, consistent with green/yellow cat's-eye chrysoberyl. Natural inclusions were observed under the microscope, as described later. For confirmation, an FTIR spectrum was collected; it showed peaks at 2163, 2403, and 4150 cm^{-1} that are characteristic of natural chrysoberyl (C.M. Stockton and R.E. Kane, "The distinction of natural from synthetic alexandrite by infrared spectroscopy," Spring 1988 *G&G*, pp. 44–46).

In this stone, we can see obvious color zoning with a fixed whitish band in the middle between transparent brownish green portions (figure 1, left). This white part is semi-transparent/translucent due to dense clouds with minute fibrous inclusions (figure 2)—these features typically cause chatoyancy in cat's-eye chrysoberyl. The cloud inclusions were not only on the cabochon surface but also located below the surface. As shown in figure 1 (right), this stone displayed distinct chatoyancy in the white zone. Even when viewed from an off-center direction, reflected light striking the clouds below the surface created the weak chatoyancy in the brownish green portions, which had no clouds or fibrous inclusions.

For the purpose of showing phenomena, stones with such localized inclusions can sometimes be oriented to place the inclusions at the base of the cabochon (Winter 2017 Lab Notes, pp. 459–460). Uneven distribution of included zones requires careful observation of the inclusion to likewise produce a good chatoyancy effect. This type of localized inclu-

Figure 1. A color-zoned cabochon measuring 16.33 × 16.07 × 10.27 mm set in a ring. Left: Distinct zoning with cloud-like inclusions is visible as a white band in the middle. Right: The stone displays chatoyancy when illuminated with fiber-optic light.

Figure 2. Dense clouds containing minute fibrous inclusions create the cat's-eye phenomenon. Larger blurry needles are visible within the cloud inclusions in the white portion. Field of view 3.0 mm.

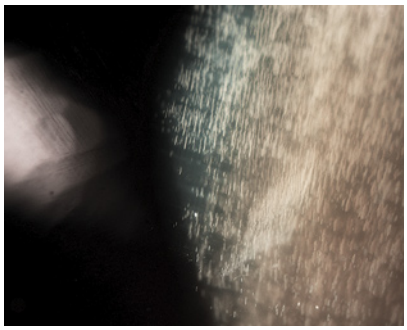

Editors' note: All items were written by staff members of GIA laboratories.

Gems & Gemology, Vol. 57, No. 4, pp. 372–381.

Figure 3. This 1.13 ct Fancy yellow diamond resembles the iconic Apple logo.

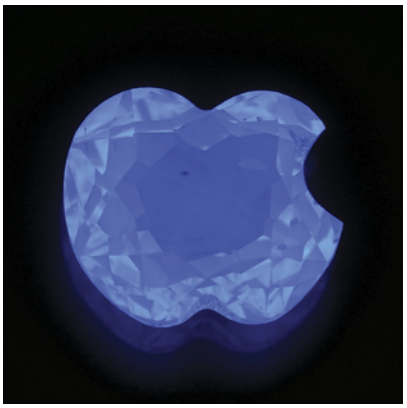

Figure 4. The novelty cut diamond showed strong blue fluorescence under long-wave UV light.

sion can sometimes lead cutters to be creative to maximize the appearance of the stone and the phenomenon.

Yusuke Katsurada

DIAMOND

Novelty Cut Diamond Faceted as Iconic Apple Logo

A novelty cut 1.13 ct Fancy yellow diamond was recently submitted to the Carlsbad laboratory for color origin and identification service. The diamond was cut in the shape of a bitten apple and bore a striking resemblance to the iconic Apple logo found on Apple Inc. products (figure 3). Standard FTIR absorption spectrum identified it as a type Ia diamond with high nitrogen concentration. Standard UV-Vis spectroscopy revealed the typical UV-Vis absorption spectra of cape diamond, with the N2 (478 nm) and N3 (415.2 nm) defects that are responsible for the fancy yellow color in the "Apple" diamond. The stone showed strong blue fluorescence when exposed to long-wave UV radiation, typical of cape diamond (figure 4).

New cutting styles of diamonds are often designed either for efficient light return and weight retention properties or to resemble other items. Examples of the latter include the sword-shaped diamond with "fire and ice" fluorescence (Fall 2020 Lab Notes, pp. 416–419) and the "seated Buddha" (Fall 1996 Gems News, p. 215). This particular diamond was most likely fashioned in the shape of an apple as a novelty and to retain weight, as the stone showed significant windowing, which suggests that the rough was too shallow to allow for more efficient light return. This unique shape for a faceted diamond is a welcome addition to the wide range of novelty cut diamonds currently available in the trade.

Maryam Mastery Salimi and Najmeh Anjomani

Two Pairs of Antique Mughal Spectacles with Gemstone Lenses

Lenses play a major role in the daily work of a gemologist, from magnification using a loupe or microscope to the optics used in conjunction with lasers from advanced testing instruments. Even our eyes contain organic lenses, which we use to see the world. In many cultures, seeing the world in completely new ways is often achievable by means of introspection such as contemplative moments or meditation, but sometimes all one truly requires is a pair of glasses.

Recently, GIA's New York laboratory had the spectacular opportunity to observe and analyze two pairs of truly unique antique spectacles (figure 5). The two spectacles have a storied connection dating back to the height of the Mughal Empire. Their lenses are crafted from diamond and emerald, respectively. According to information provided by the client and independent researchers, the two pairs of spectacles were likely fashioned in mid-seventeenth century

Figure 5. These antique spectacles contain diamond (left) and emerald (right).

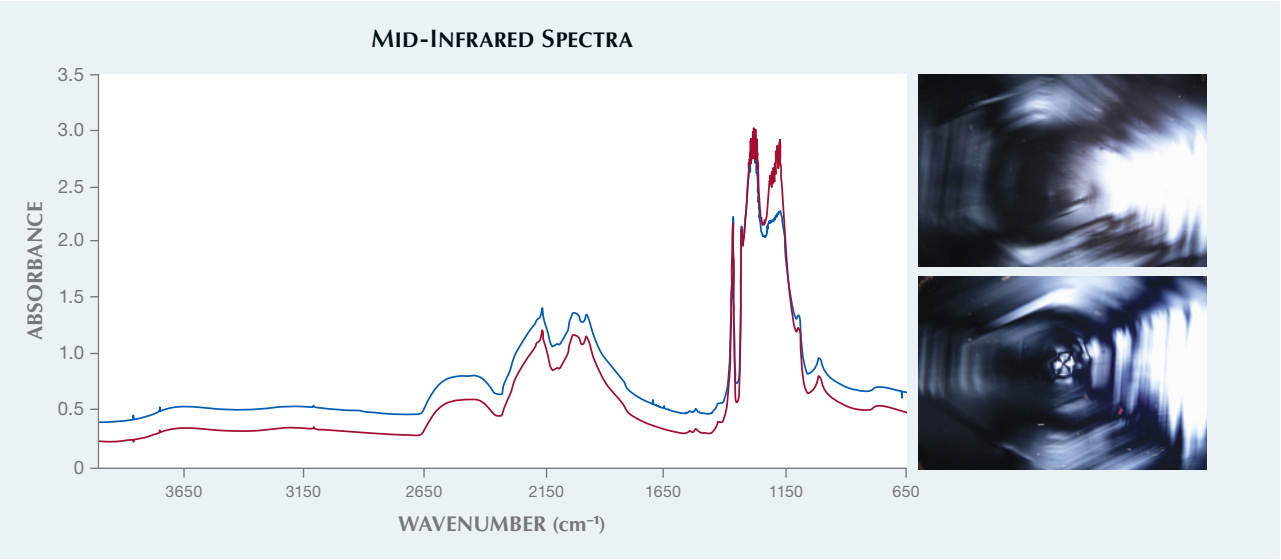

Figure 6. Left: Overlapping mid-infrared spectra of both lenses revealed them to be type Ia diamonds. Right: Two strain images, one of each lens, under cross-polarized light showing natural growth structure and internal stress during natural diamond formation. Field of view 19.27 mm.

India, a period in the Mughal Empire that had an established lapidary tradition and artisans with the expertise to accomplish such creations. Information submitted by the client suggests that the lenses may have been cut from the same rough diamond and the same rough emerald, respectively. Further evidence suggests that while the fashioning of the lenses dates back to the seventeenth century, the frames date from the late nineteenth century based on design and style.

The first of the two spectacles, called Halqeh-Ye Nur or "Halo of Light," consists of two transparent near-colorless modified pear-shaped lenses in a yellow metal frame surrounded by numerous transparent near-colorless stones of various shapes and cuts. The client requested that only the two near-colorless transparent lenses be tested. Infrared spectra and strain images were collected as part of the testing (figure 6). Both lenses were identified as natural type Ia diamonds, sharing matching spectra when overlapped. The strain images revealed natural growth structures and internal stress during diamond formation. While GIA's investigations were limited in scope to identifying the gem material set in each pair of spectacles, the evidence as a whole seems to suggest that the lenses were cleaved from the same large diamond rough.

The second pair of spectacles, called Astaneh-Ye Ferdaws or "Gate of Paradise," consists of two transparent green pear-shaped lenses in a white and yellow metal frame set with two green rectangular step cuts and numerous near-colorless stones of various shapes and cuts. According to information provided by the client, the pear-shaped lenses originate from a single natural emerald that originally weighed more than 300 carats. Both spectacles are consistent with the design and style of the late nineteenth century and are believed to have been upgraded to the fashion of the time.

Figure 7. A field of jagged three-phase inclusions hosting gas bubbles, colorless cubic crystals, and aqueous liquid. Field of view 1.99 mm.

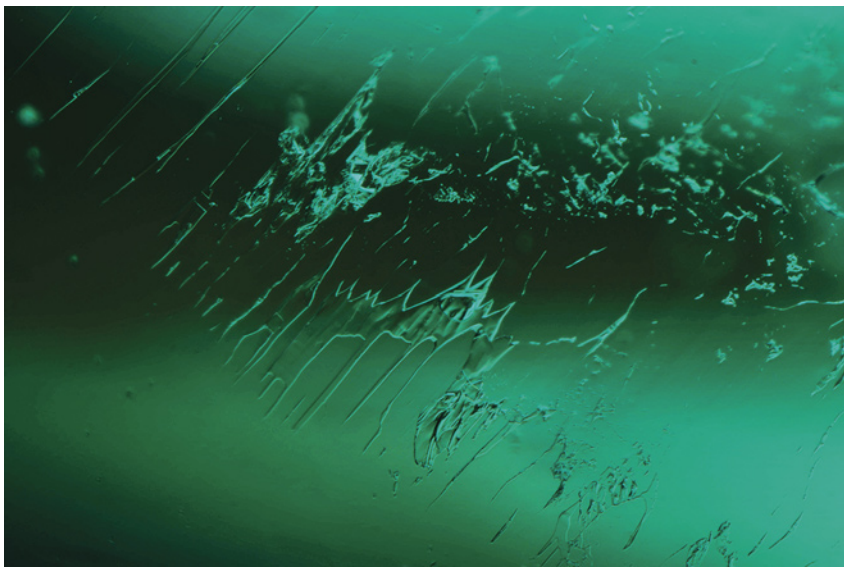

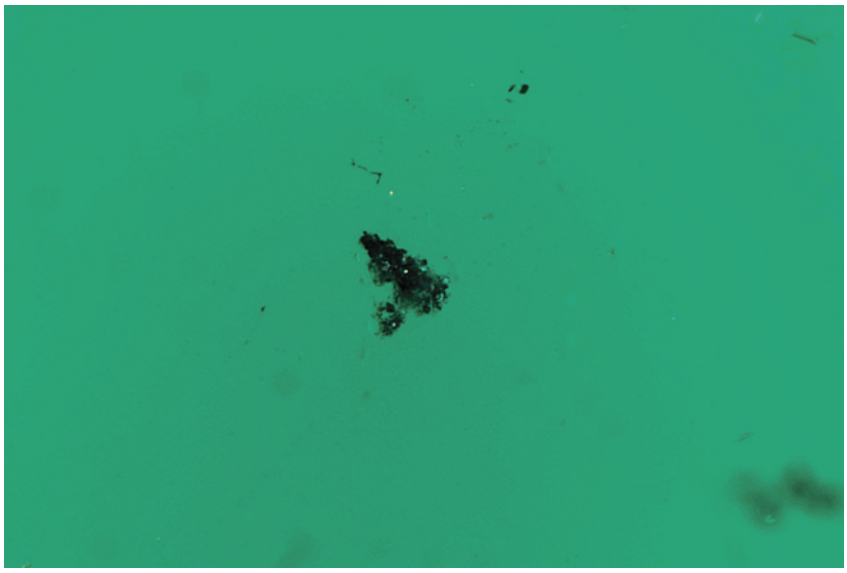

Figure 8. Opaque black grains were also observed, consistent with inclusions observed in emeralds from Colombia. Field of view 1.26 mm.

The client requested that both green transparent lenses as well as all 45 of the surrounding near-colorless stones be tested. Microscopic observation, one of the main identification methods for emeralds, revealed an inclusion scene typical for emeralds from Colombia: classic jagged three-phase inclusions hosting a gas bubble and a cubic colorless crystal suspended in fluid (figure 7). It is well established that these daughter crystals are halides, commonly rock salt, derived from the saline brine contained in the primary fluid inclusion (E.J. Gübelin and J.I. Koivula, *Photoatlas of Inclusions in Gemstones*, Vol. 3, 2008, Opinio-Verlag Publishers, Basel, Switzerland, p. 427). Unidentified tiny opaque black grains were also observed (figure 8), but otherwise the lenses were relatively inclusion free. Examination of minor fissures seen near the gem's surface using ultraviolet light and microscopic observation indicated the presence of an oil or resin, but this is not believed to have affected the overall appearance. Therefore, the emeralds were classified as having "no indications of clarity enhancement."

Standard gemological testing revealed a refractive index of 1.577 to 1.583 with a birefringence of 0.006. Examination between crossed polarizing filters showed a uniaxial optic figure. The pleochroism was green to blue-green, and a handheld spectroscope revealed a typical emerald spectrum. These properties and observations confirmed that the green transparent lenses were natural emeralds.

All 45 of the transparent near-colorless stones surrounding the two emerald lenses were identified as diamonds using GIA's iD100 device, microscopic observation, and additional advanced testing.

Even by today's standards, these astonishing curiosities are objects of technical mastery by the artisans and the brilliant vision of the patrons who commissioned the spectacles. From these fine examples of Mughal craftsmanship, to more modern examples such as synthetic sapphire sunglasses made for Sir Elton John (see Winter 1997 Lab Notes, p. 296), we continue to be pleasantly surprised by gem materials passing through GIA that have been fashioned into unique items such as these lenses. We imagine Sir Elton would approve of these Mughal spectacles.

Christopher Vendrell, Augusto Castillo, and Emily Jones

Pink EUCLASE

GIA's Tokyo laboratory had the opportunity to examine an orangy pink faceted stone, weighing 4.08 ct and measuring 13.00 × 9.90 × 5.23 mm, with a hydrostatic specific gravity of 3.09 (figure 9). It had optically biaxial features based on trichroic colors of yellowish orange, pale orange, and orangy pink, and refractive index values of 1.652–1.671 with a birefringence around 0.019. The stone was inert to ultraviolet light sources.

Figure 9. The 4.08 ct orangy pink euclase. Parallel pink color zoning is observed under the table.

Transparent platy crystals and straight graining were observed under the microscope (figure 10). There were no signs of treatment such as coating or clarity enhancement. Gemological properties matched euclase, which was confirmed by comparing the Raman spectrum with the RRUFF database (reference spectrum R050032).

Euclase is one of several collector's minerals discovered in the eighteenth century in Brazil (D. Atencio, "The discovery of new mineral species and type minerals from Brazil," *Brazilian Journal of Geology*, Vol. 45, No. 1, 2015, pp. 143–158) and classified as a beryllium aluminum hydroxide silicate, with an ideal chemical formula of $BeAlSiO_4(OH)$. Crystals are found worldwide and occur in a range of colors such as colorless or white, blue, green, and yellow (e.g., S.M. Stocklmayer, "A new occurrence of euclase in Western Australia," *Australian Journal of Mineralogy*, Vol. 18, No. 2, 2017, pp. 39–44). Gem-quality pink euclase was first reported in 2018 (M.B. Leybov, "Denver 2018: 'Minerals of Mexico,'" *Mineralogical Almanac*, Vol. 24, No. 1, pp. 58–63), and this color is considered rare.

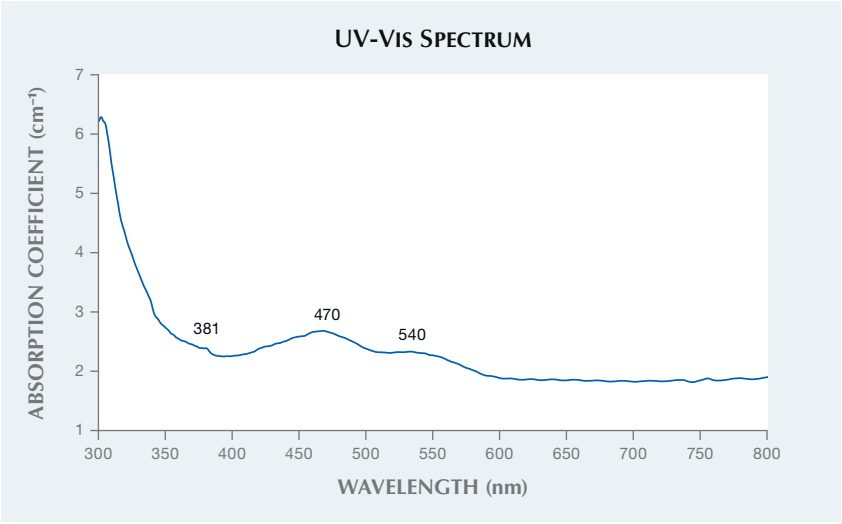

Figure 11. UV-Vis spectrum of this orangy pink euclase. The 470 and 540 nm absorption peaks probably originated from Mn^{3+} and the 381 nm peak from Fe^{3+}.

The causes of color for euclase have been discussed in many studies (e.g., E. Gübelin, "Sapphire-blue euclase, a new collector's gem," Winter 1978-1979 *G&G*, pp. 104–110; M. Mattson and G.R. Rossman, "Identifying characteristics of charge transfer transitions in minerals," *Physics and Chemistry of Minerals*, Vol. 14, No. 1, 1987, pp. 94–99; S. Stocklmayer, "Blue euclase from Zimbabwe – a review," *Journal of Gemmology*, Vol. 26, No. 4, 1998, pp. 209–218). According to these three previous studies, blue to green color in euclase is believed to be caused by an Fe^{2+}-Fe^{3+} charge transfer and Fe^{2+}-Ti^{4+} transitions or the presence of trivalent iron. Moses et al. (Summer 1993 Gem Trade Lab Notes, pp. 125–126) reported a greenish blue euclase colored by chromium. Gilles-Guéry et al. ("Mn^{3+} and the pink color of gem-quality euclase from northeast Brazil," *American Mineralogist*, 2021, in press) determined that pink coloration due to the absorption between green to blue with two broad peaks at 470 and 540 nm is caused by Mn^{3+}, while the orange hue is related to the rising slope in the UV domain combined with an additional absorption peak at 381 nm originating from Fe^{3+}. This stone showed a UV-Vis absorption spectrum (figure 11) similar to the pattern due to Mn^{3+} reported by Gilles-Guéry et al. (2021), and trace Mn concentrations around 60 ppm were detected by LA-ICP-MS. These characteristics suggest that the orangy pink color seen in this stone is possibly caused by manganese. This is the first such example examined at GIA.

Figure 10. Transparent platy crystal inclusions and aligned particles were observed. Field of view 1.85 mm.

Mari Sasaki, Makoto Miura, and Kazuko Saruwatari

Figure 12. Single-strand freshwater bead cultured necklace measuring 10.33 × 10.18 mm to 13.36 × 12.72 mm.

Figure 14. X-ray fluorescence analysis of the strand showed a yellowish green reaction along with a reddish orange reaction on the irregular white patches.

Vaterite Found on a Strand of Freshwater Cultured PEARLS

Recently, GIA's New York laboratory received a single-strand necklace with 32 pearls for identification (figure 12). The pearls were white and near-round, ranging from 10.33 × 10.18 mm to 13.36 × 12.72 mm in size and weighing 81.50 grams total. Real-time microradiography (RTX) analysis revealed that all of them had a bead nucleus. Chemical analysis by EDXRF spectrometry showed a high manganese concentration and low strontium, indicating they formed in a freshwater environment. During examination of the strand, random white patches were observed on the surface of many of the pearls. These irregular patches appeared overgrown on the surface and crystalline-like (figure 13).

X-ray fluorescence analysis revealed a strong yellowish green reaction around each pearl, while the irregular white surface patches showed a reddish orange reaction with moderate intensity (figure 14).

Additionally, Raman analysis of the nacreous surface and the irregular white patches revealed they consisted of two calcium carbonate polymorphs: aragonite and vaterite, respectively (figure 15). Aragonite peaks were ob-

Figure 13. Irregular whitish patches were visible on the surface of many of the pearls.

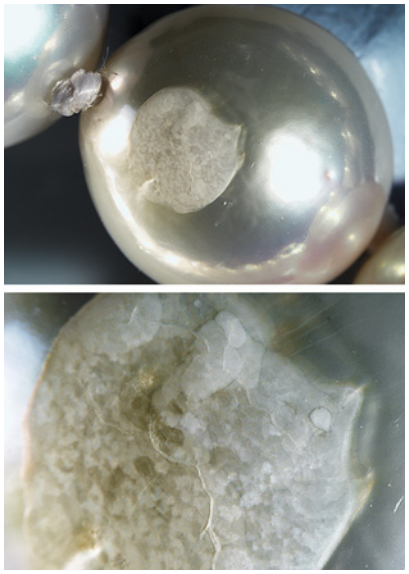

Figure 15. Raman analysis found aragonite peaks at 701, 704, and 1085 cm^{-1} and vaterite peaks at 740, 750, 1075, and 1090 cm^{-1}.

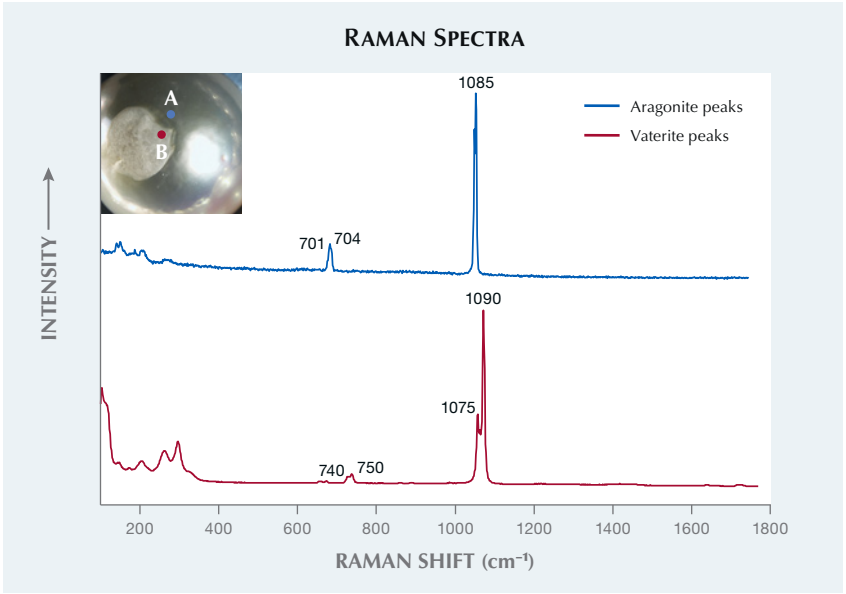

served at 701, 704, and 1085 cm^{-1}; vaterite peaks were at 740, 750, 1075, and 1090 cm^{-1}.

Formation of the shells and pearls relies on the epithelial cells of the mollusk. Aragonite and calcite are the two most common calcium carbonate polymorphs found in pearls, while vaterite is the third most common and also the least stable form. Vaterite has only been found in freshwater pearls so far (Li Qiao et al., "Special vaterite found in freshwater lackluster pearls," *Crystal Growth & Design*, Vol. 7, No. 2, 2007, pp. 275–279; Summer 2021 Gem News International, pp. 171–174). Although the reason why vaterite formed on the pearls' surface is unknown, the defect is one of the most unusual formations seen, especially in an entire strand.

Sally Chan Shih

Figure 16. This 19.44 ct orangy pink rhodochrosite contains a four-rayed star.

Star RHODOCHROSITE

The Carlsbad laboratory received a 19.44 ct semitransparent orangy pink round cabochon for identification (figure 16). With the unaided eye, a four-rayed star could be seen across the dome. Standard gemological properties, including a refractive index of 1.68–1.58 with a birefringence blink and a specific gravity of 3.71, were documented and consistent with the gem species rhodochrosite.

Asterism is created when light is reflected off well-aligned inclusions and returns as a star across the surface of the stone. Such stones are commonly cut as cabochons to properly display this phenomenon. The asterism seen in this rhodochrosite was created from fluid inclusions that run parallel to the base of the cabochon (figure 17). The fluid inclusions were rhomboid in shape, which caused the star to have four rays. It is worth noting that the rays of the star did not cross perpendicular to each other, and this is due to the rhomboid fluid inclusions intersecting at an angle not at 90°.

Many gemstone species display asterism, but this was the author's first opportunity to see a star rhodochrosite. This 19.44 ct stone is a perfect example of why one should always keep an eye out for the unexpected.

Nicole Ahline

Figure 17. Fluid inclusions in a step-like pattern running parallel to the base of the rhodochrosite cabochon. Field of view 4.14 mm.

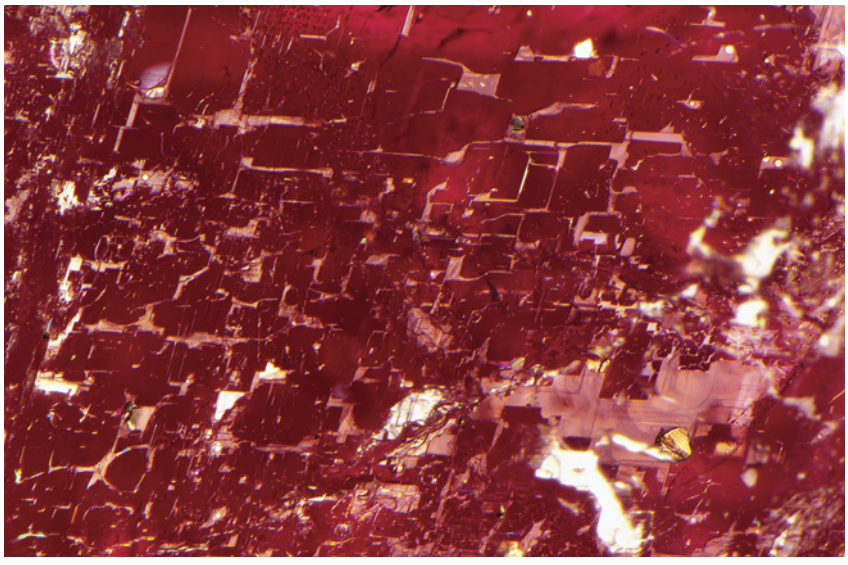

Exceptionally Large and Well-Saturated Orange SAPPHIRE

The Carlsbad laboratory recently received an exceptionally large orange cushion mixed-cut sapphire weighing 31.06 ct (figure 18) submitted for an identification and origin report. Stan-

Figure 18. 31.06 ct well-saturated orange sapphire measuring 18.65 × 13.85 × 11.81 mm.

dard gemological testing gave a refractive index of 1.769–1.762 and a hydrostatic specific gravity of 3.98, indicating corundum. This sapphire exhibits a saturated orange color that is attributed to the trace element magnesium in the stone's crystalline structure. Microscopic examination showed altered crystals with healing and irregular bands of particles. These altered inclusions suggest that the stone underwent heat treatment. Internal characteristics similar to these are often found in sapphires from deposits of metamorphic sources. Laser ablation–inductively coupled plasma–mass spectrometry (LA-ICP-MS) confirmed the stone had a lower content of trace element iron. The chemistry and internal features of this gemstone indicate an origin of Sri Lanka.

Rough material that will cut large, high-quality sapphires is rare, with most finished stones being less than five carats. Fine gem-quality examples of more than ten carats are considered very rare. The combination of a large size and a well-saturated orange color makes this 31.06 ct sapphire a notable gemstone.

Jessa Rizzo

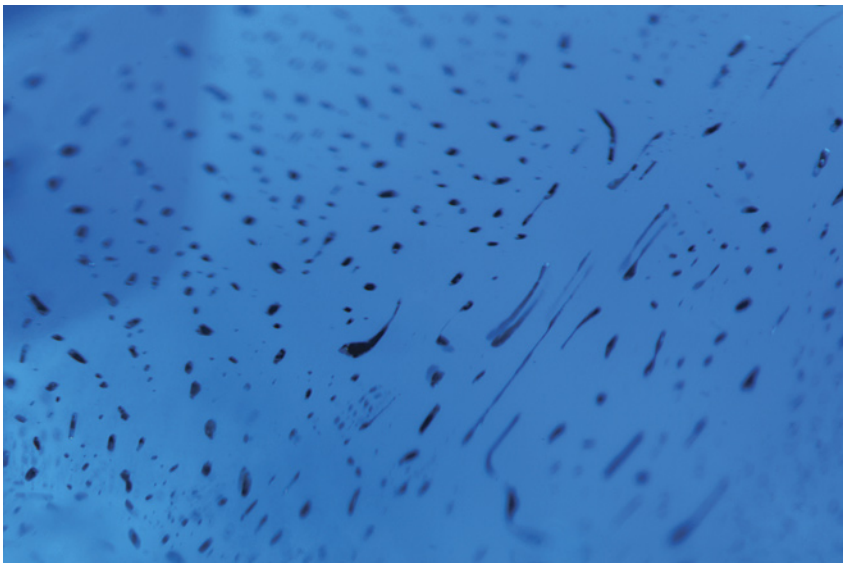

Figure 20. This flux fingerprint in the lab-grown sapphire is similar to the fingerprints found in natural sapphire. Field of view 1.76 mm.

Flux-Induced Fingerprints in Flame-Fusion SYNTHETIC SAPPHIRE

The Carlsbad laboratory recently received a blue cushion mixed cut measuring 9.07 × 7.07 × 4.62 mm (figure 19). Standard gemological testing gave a refractive index of 1.760–1.768, consistent with sapphire. Microscopic examination uncovered a fingerprint resembling those found in natural sapphires (figure 20). Closer examination revealed the fingerprint to be a flux fingerprint. When the stone was immersed in mineral oil, curved color banding diagnostic of flame-fusion lab-grown sapphire became visible (figure 21).

Typically, a flame-fusion-grown

Figure 19. Face-up view of the 2.81 ct flame-fusion synthetic sapphire with flux fingerprints.

Figure 21. When immersed in mineral oil, curved color banding is visible along with a natural-looking flux fingerprint and large gas bubbles. Field of view 7.19 mm.

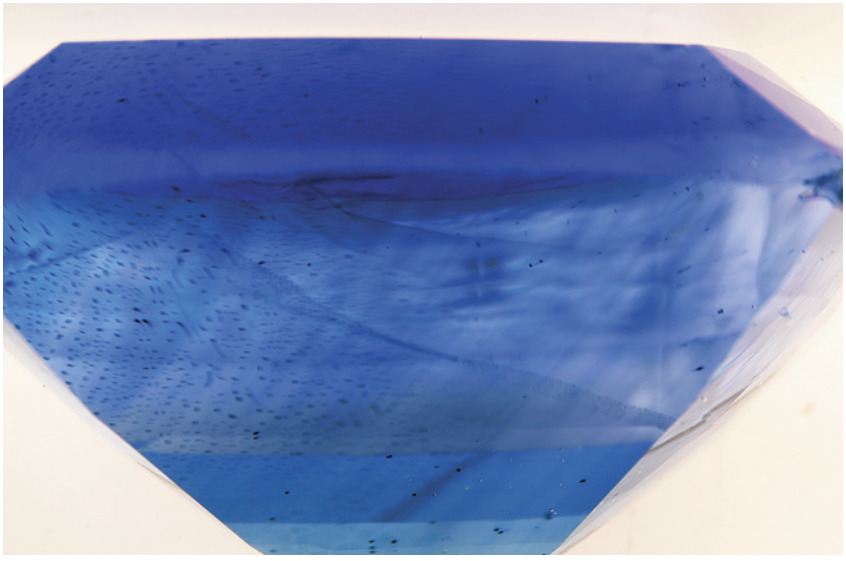

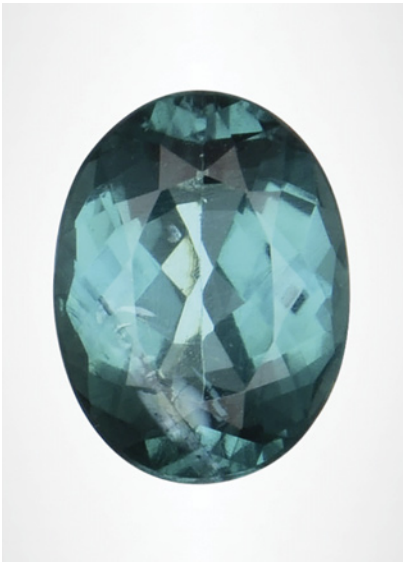

Figure 22. This 0.70 ct tourmaline shows unique surface patterns.

ruby or sapphire with healed fractures has undergone a process known as "quench crackling," where fractures are created in the stone by heating and subsequent rapid cooling. This stone did not show the characteristic cellular fracturing created by this process, making the healed fractures appear even more natural. The randomly fractured stone had been immersed in a flux melt. The flux melt filled and partially healed the fractures while the stone gradually cooled, which resulted in natural-looking fingerprints of residual flux. This treatment is usually seen in flame-fusion synthetic rubies (K. Schmetzer and F.-J Schupp, "Flux-induced fingerprint patterns in synthetic ruby: An update," Spring 1994 *G&G*, pp. 33–38).

Michaela Stephan

Unique Circuit Board–Like Surface Pattern on TOURMALINE

The Tokyo laboratory recently received a 0.70 ct blue-green oval modified brilliant measuring 6.62 × 4.99 × 3.10 mm (figure 22). Standard gemological testing yielded a refractive index of 1.620–1.640, uniaxial interference pattern, and a hydrostatic specific gravity of 3.10, all consistent with tourmaline. No Cu was detected with energy-dispersive X-ray fluorescence (EDXRF). UV-Vis-NIR spectrometry did not show Cu absorption bands but did show a strong Fe absorption. This stone, therefore, did not meet the requirement to be designated as a Paraíba tourmaline, whose dominant coloring agent of green/blue must be Cu (LMHC Information Sheet #6, 2012).

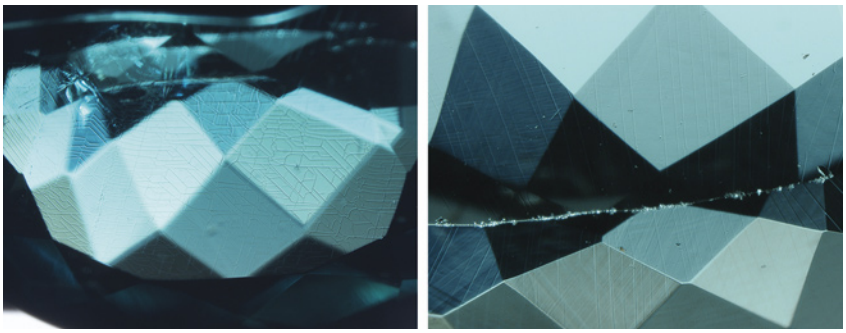

Figure 23. The circuit board–like features point mainly in three directions on the crown (left) and are aligned in only one direction on the pavilion (right). Field of view 3.95 mm (left) and 2.91 mm (right).

Microscopic observation revealed a unique networked pattern, resembling the pattern of a circuit board, covering the overall surface of the stone. The surface features mainly pointed in three directions on the crown but did not show a clear three-directional pattern on the pavilion (figure 23). Viewed under reflected

Figure 24. Some features on the table facet, photographed in reflected light, were parallel to the polish lines. Field of view 3.80 mm.

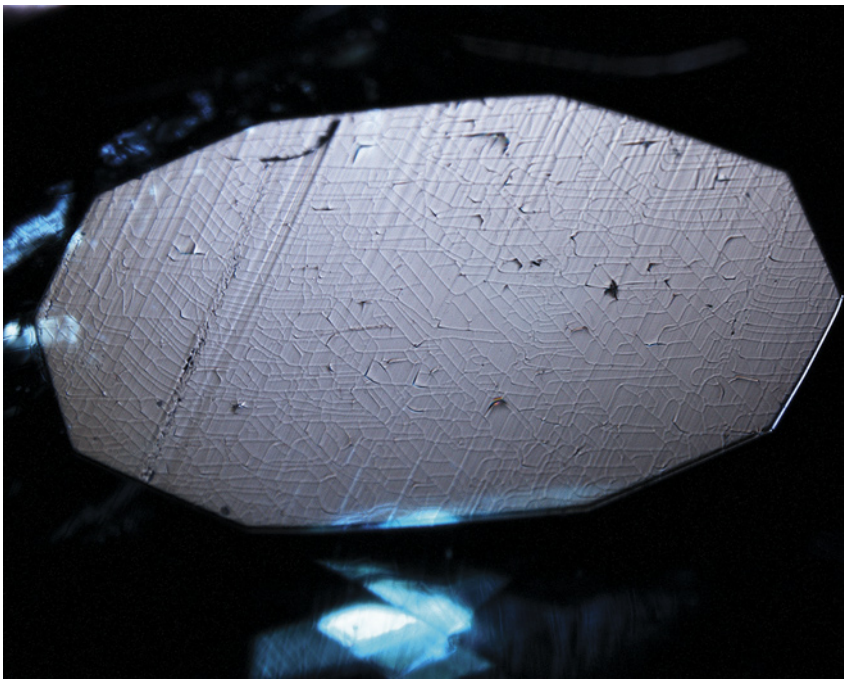

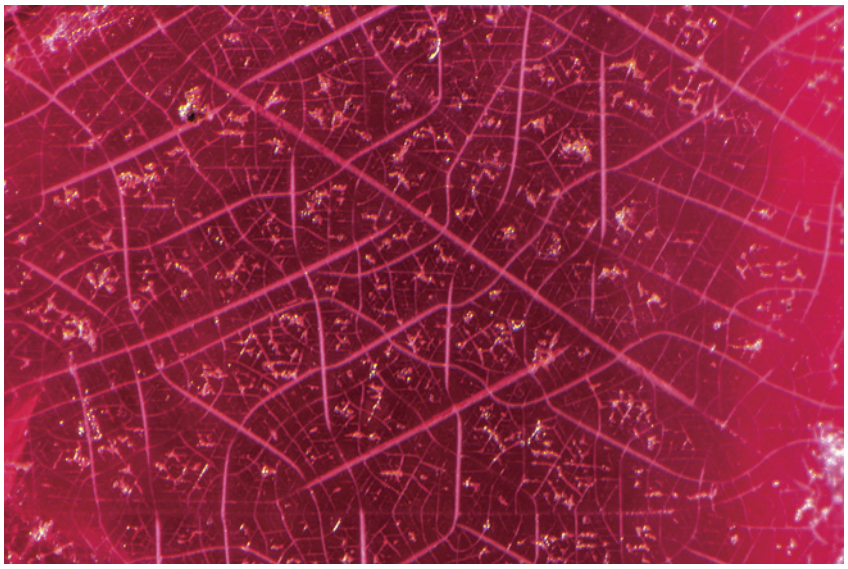

Figure 25. Features similar to the tourmaline's superficial fractures have been seen on the surface of rough crystals such as this Burmese spinel with fractures that likely result from strain in the crystal lattice. Field of view 2.35 mm.

light, some features at the table facet were parallel to the "polish lines" (figure 24). No evidence of coating and no color concentration along the pattern were found. The conoscope image with crossed polarized filters showed that the table facet was perpendicular to the c-axis. Because tourmaline belongs to the trigonal crystal system, the features appeared to be crystallograpically aligned. That could also explain why the patterns were different between the crown and the pavilion.

We also observed tension cracks surrounding fluid inclusions, which indicated the possibility of heat treatment. In addition, this color of tourmaline is commonly heat treated to improve its color.

Because the unique patterns were related to the crystal structure, they may have been caused by thermal shock related to heat treatment and/or acid etching. Similar crystallographically aligned surface features have been found on rough crystals of Tanzanian tourmaline and Burmese spinel (figure 25; N. Renfro, pers. comm., 2021). What caused this pattern and how it came to be revealed on a faceted stone remains a mystery. More samples and further experiments are needed to unravel the cause of these unique and interesting patterns.

Yuxiao Li and Yusuke Katsurada

PHOTO CREDITS
Shunsuke Nagai—1, 9, 22; Yusuke Katsurada—2; Diego Sanchez—3, 4, 16, 18, 19; Jian Xin (Jae) Liao—5; Christopher Vendrell—6; Augusto Castillo—7, 8; Mari Sasaki—10; Sood Oil (Judy) Chia—12; Sally Chan Shih—13, 14; Nicole Ahline—17; Nathan Renfro—20, 21, 25; Michaela Stephan—20, 21; Yuxiao Li—23, 24